International Journal of Pharmaceutical and Bio-Medical Science
ISSN(print): 2767-827X, ISSN(online): 2767-830X
Volume 03 Issue 03 March 2023
Page No: 115-124
DOI: https://doi.org/10.47191/ijpbms/v3-i3-05, Impact Factor: 6.858

Computational Methods to Unveil the Structural Bases for the Recognition of SARS-Cov-2 by Human Nicotinic Acetylcholine Receptors

Ottavia Spiga[1,2,3], Luisa Frusciante[1], Michela Geminiani[1,2], Francesco Pettini[1], Alfonso Trezza[1], Anna Visibelli[1], Annalisa Santucci[1,2,3]

[1]Department of Biotechnology, Chemistry and Pharmacy, University of Siena, Via A. Moro 2, 53100 Siena, Italy
[2]SienabioACTIVE - SbA, 53100 Siena, Italy Competence Center ARTES 4.0, Siena, Italy
[3]Competence Center ARTES 4.0, 53100 Siena, Italy

ABSTRACT

The novel pathogen SARS-CoV-2 has caused the global pandemic of Covid-19. The hypothesis of this study is that Nicotinic Acetylcholine Receptors (nAChRs) are involved in SARS-CoV-2 infection, explaining the hyper-inflammatory characteristics observed in a subset of Covid-19 patients. nAChRs represent specific receptors for a wide variety of toxins and have been proposed to serve as receptors for Rabies Virus (RABV) and Human Immunodeficiency Virus (HIV) as well, based on sequence homology with the so called "toxic loop" of α-bungarotoxin. Sequence similarities between a motif found in SARS-CoV-2 S protein and in snake neurotoxins, as well as RABV neurotoxin-like region, HIV-1 gp120 and α-conotoxin from Conus geographus, highlights the existence of a correlation between these proteins' functional sites. In this study, in silico procedures were used to determine SARS-CoV-2 S protein structure-function relationships, revealing the presence of features characteristic of the "toxic loop" known to bind nAChRs and their involvement in the S protein-nAChR interaction. Our results suggest that a polybasic sequence-carrying motif found in SARS-CoV-2 S protein could be involved in the binding, in particular underling the role of Arg685 in the interaction with the receptor.

KEYWORDS: Nicotinic Receptor; Covid-19; SARS-CoV-2; Rabies Virus; HIV-1.

ARTICLE DETAILS

Published On:
10 March 2023

Available on:
https://ijpbms.com/

INTRODUCTION

Since December 2019, the first cases of pneumonia associated with a new virus, SARS-coronavirus 2 (SARS-CoV-2), were identified by the Chinese authorities in Wuhan, Hubei province, China[1] On February 21, 2023, 757.264.511 confirmed cases had been documented worldwide [2], with clinical manifestations ranging from mild or no symptoms to severe illness, being identified as viral pneumonia [3]. The entry of SARS-CoV-2 into target cells is mediated by the Spike protein (S) which is responsible for interacting with host cell receptor Angiotensin-Converting Enzyme (ACE2) following the priming of S protein by specific proteases at S1/S2 and the S2' sites [4]. Clinical manifestations of Covid 19 infection include viral pneumonia, symptoms such as fever, cough, and chest discomfort, as well as dyspnea and bilateral lung infiltration in severe cases [3]. Critically ill patients displayed lymphocytopenia, neutrophilia, low numbers of monocytes, eosinophils, and basophils, as well as high levels of inflammatory mediators and infection-related indicators. Evidence suggests that a cytokine storm, pathogenic immune response

characterized by an excessive, dysregulated production of cytokines in response to infection, plays a role in the severity of the Covid-19 disease leading to multi-system inflammatory syndrome (MIS-C), or COVID-19 hyperinflammation [5].

SARS-CoV-2 S protein carries a polybasic insertion that was absent in SARS-CoV [6]. Based on sequence homology with the loop II of α-neurotoxins, the so-called "toxic loop", hypotheses have been put forward of possible interaction of this sequence motif with Nicotinic Acetylcholine receptors (nAChRs), which could explain the hyper-inflammatory characteristics observed in a subset of Covid-19 patients [7]. nAChRs belong to the superfamily of Cys-loop pentameric ion channels, a large group of proteins with diverse functions involved in excitatory and inhibitory signaling. As ligand-gated cation channels, they specifically mediate fast excitatory neurotransmission and are activated by the neurotransmitter acetylcholine (ACh). In humans, 17 different subunits, α1-α10, β1- β4, γ, δ, and ε in different combinations form distinct subtypes of functional channels, differentiated by composition and localization [8]. Mainly they are found at the cerebral, muscular, and ganglia levels; however, nAChRs have also been found at the peripheral level, including immune cells [9]. The innate immune system serves as the initial defense line against invasive pathogens, and cholinergic signaling via the efferent vagus nerve finely regulates the immunological activity and pro-inflammatory reactions. Increased release of ACh from the vagus nerve in response to endogenous or exogenous stimuli triggers the activation of nAChRs on the macrophage cell membrane, reducing the production of inflammatory cytokines and, as a result, inhibiting inflammation [10].

nAChRs play a role not only in physiological functions but also serve as specific ligands for a wide variety of molecules and toxins that are known to target the receptor as a defense mechanism, among other things. Natural molecules interacting with nAChRs include the natural alkaloid nicotine and nAChR antagonists like curare alkaloids [11]. Among the animal toxins able to target these receptors, snake and cone snail venoms are the more widely characterized. These toxins are selective inhibitors of nAChRs able to compete with ACh for binding to the receptor binding site [12]. Different neurotoxins have been sequenced and a comparison of their primary structures as well as studies on their three-dimensional conformation provided useful information about nAChRs interactions with ligands and pharmacology. These α-neurotoxins are small proteins and peptides and include α-bungarotoxin and α-conotoxin, characterized by the presence of a common "toxic loop" structure able to bind different subtypes of the neuronal nAChRs [11,13]. nAChRs have been proposed to serve as receptors for Rabies Virus (RABV) as well, and several studies have devised the involvement of these ion channels in Human Immunodeficiency Virus (HIV) infection [13,14]. RABV cell entry mechanisms involve 400 trimeric spikes on the ectodomain of the virus glycoprotein (RABVG) [15], the protein accountable for interacting with nAChRs since RABVG shares homologous sequences with the "toxic loop" of α-bungarotoxin [16]. The interaction with nAChRs is accountable for the central symptoms of the infection, characterized by hallucinations, respiratory problems, muscle spasms, and even paralysis [17]. A comparable homology with neurotoxins loop II is also found in the sequence of HIV-1 envelope glycoprotein 120 (gp120) [13]. Several studies report the nAChR as an important player in HIV infection since it is expressed not only in the brain, but also in macrophages, monocytes, B-lymphocytes, and T-lymphocytes (CD4+) [18–20], all cell types involved in HIV infection.

Several studies have devised the involvement of nAChRs in Covid-19 pathophysiology [5,21–27]. In this work, *in silico* procedures were used as a basis to determine the structure-function relationship of the SARS-CoV-2 S protein. The involvement of specific amino acid residues in the interaction with nAChRs was predicted using sequence and structure analysis.

RESULTS

Here is reported a sequence comparison between the polybasic sequence-containing region found in SARS-CoV-2 S (675-QTQNSPRRAR-685) and the "toxic loop" of α-bungarotoxins and RABV neurotoxin-like region, as well as HIV-1 gpl20 and α-conotoxin from *Conus geographus* (Figure 1).

SARS-CoV-2 S (675-685)	QTQTNSPRRAR
α-bungarotoxin (50-60)	CDAFCSSRGKV
RABVG(CVS-11) (214-224)	SRGKRASKGNK
HIV-1 gp120 (159-169)	FNISTSIRGKV
α-conotoxin (2-12)	CCNPACGRHYS

Figure 1. Sequence comparison between SARS-CoV-2 S (P0DTC2), α-bungarotoxin (P60615); RABVG (O92284); HIV-1 gpl20 (P04578) and α-conotoxin (P01519). Red-boxed amino acids represent the putative binding sites comprehending positively charged residues that could interact with the receptor.

To gain molecular insights into the possible interaction of SARS-CoV-2 with nAChRs, we studied the structures of known ligands of the receptor and compared them with the SARS-CoV-2 S protein. Since the polybasic 682-RRAR-685 motif coordinates were missing from all available crystal structures, molecular modelling was performed to predict the 3D structure of this region. The homology model of the selected HIV-1 gp120 (P04578) putative nAChR binding region was carried out as well and is shown in Figure 2, along with SARS-CoV-2 S and the binding regions of α-bungarotoxin, RABVG, and α-conotoxin. All the proteins, except for α-conotoxin, share a typical fold characterized by three β-sheeted loops, comprehending the toxic loop II carrying the positively charged amino acid residues involved in the interaction with the receptor.

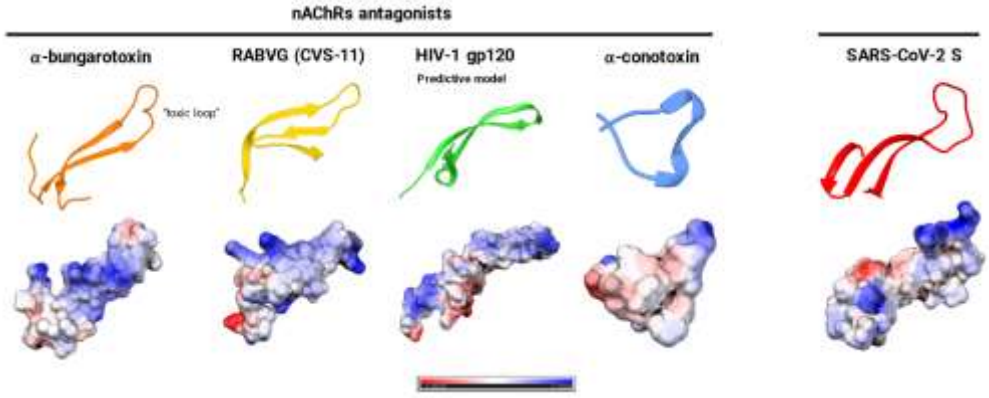

Figure 2. Structure comparison between SARS-COV-2 S protein putative nAChR binding site and known ligands of nAChRs. Electrostatic potential calculations are reported. The range of electrostatic surface potential is shown from -2 kT/e (red color) to +2 kT/e (blue color).

Examination of the electrostatic potential surfaces mapped to the molecular surface of the putative binding regions of SARS-CoV-2 S protein, α-bungarotoxin, RABVG, HIV-1 gp120, and α-conotoxin indicates positively charged areas (Figure 2). A comparison of the molecular surfaces calculated for selected loops shows that although the residues forming the loop are not the same, as is the case for α-bungarotoxin and HIV-1 gp120, the electrostatic potential surfaces are very similar. Therefore, the surface properties of the regions of these proteins should be similar to those of α-bungarotoxin. Thus, the surface properties of these proteins' regions would be expected to be similar to those of α-bungarotoxin. We further report the electrostatic potential surface map for the nAChR α9-subunit, which shows a negatively charged area surrounding the loop-C of the receptor, known to interact with α-bungarotoxin (Figure 3a).

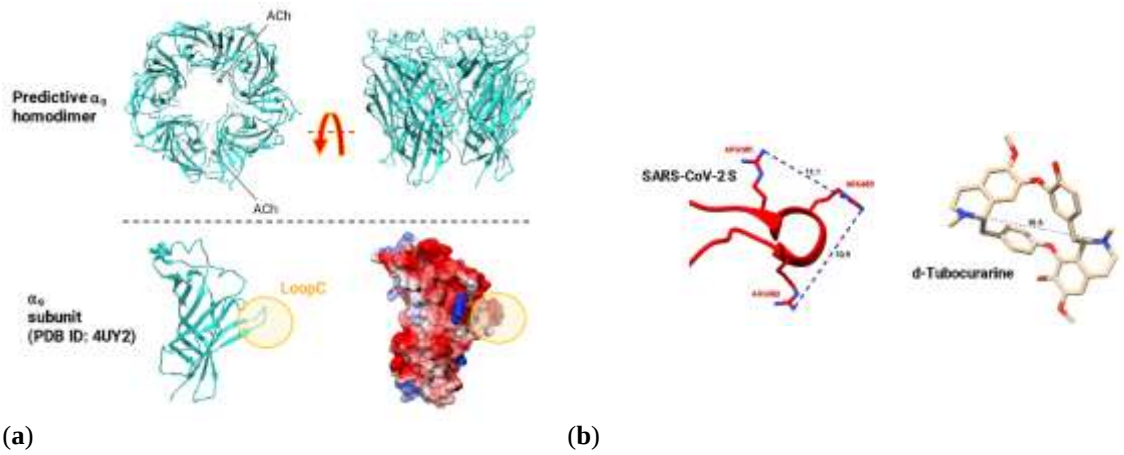

(**a**) (**b**)

Figure 3. (a) nAChR α9-subunit binding site. Loop C structure and electrostatic potential were circled in yellow. The range of electrostatic surface potential is shown from -2 kT/e (red color) to +2 kT/e (blue color). (b) SARS-CoV-2 S hairpin portion (red); d-Tubocurarine (gold) in the binding to the Acetilcholine Binding Protein (AChBP) from Aplysia californica (not shown; PDB ID:2XYT).

It is known that two molecules of ACh are needed to bind the nAChR to activate the ion channel. The binding of agonists or antagonists, like the members of the curare family, to the receptor, is linked to the presence of two positively charged atoms at a distance comprised between 9-11 Å which is the distance assumed by the charged ammonium groups of the two ACh molecules spanning two subunit interfaces in the interaction [28]. Figure 3b shows the distance between the charged ammonium groups of the nAChRs antagonist d-Tubocurarine compared to the distance assumed by the guanidinium groups of the modelled hairpin of SARS-CoV-2 S protein. The three Arg residues are located at a distance of 9-11 Å (Figure 3b), indicating a favorable conformation to be engaged in the interaction with the receptor. Taken together, these observations suggest a functional convergence between these different proteins.

To predict the structure of the interacting complex, we integrated homology modeling and molecular dynamics (MD) simulations with the molecular binding information obtained previously. The modelled loop was inserted in the available crystal structure of the SARS-CoV-2 S protein (PDB ID: 6VYB). The starting point was the α-bungarotoxin in its binding conformation with the α9-nAChR subunit (Figure 4a).

(**a**) (**b**)

Figure 4. (a) α-bungarotoxin (orange) in the binding mode with the α-9 nAChR subunit (cyan, PDB ID:4UY2); (b) the modelled loop of SARS-CoV-2 S protein (red) in the same binding mode with the α-9 nAChR subunit (cyan) after MD simulation.

The interaction between the 675-QTQNSPRRAR-685 region of the SARS-CoV-2 S putative binding loop and the so called "aromatic box" of α9-nAChR subunit in the binding conformation with α-bungarotoxin was evaluated after performing MD simulations (Figure 4b).

Modeling the SARS-CoV-2 hairpin region was a critical step that required very accurate refinement work. Upon manually binding the hairpin to the two beta-strands, it was observed that the only possible conformation is the one in which, of the three Arg residues found in the cationic moiety of SARS-

CoV-2 S, Arg685 is the one inserted into the α9-nAChR subunit "aromatic box" (Figure 4b). Residue interaction Network (RIN) analysis revealed that Arg685 interacts via a cation-π interaction with Tyr199, is engaged in Van der Waals interactions with Tyr192 and Tyr195, and interacts by H-Bond with Tyr95 of the α9-nAChR subunit, suggesting a quite stable interaction (Table 1).

Table 1. Residue-interaction network (RIN) of Arg685 from the putative binding loop of SARS-CoV-2 S protein, with nodes and edges representing interacting residues and non-covalent interactions, respectively.

NodeId1	Interaction	NodeId2
685:ARG	HBOND:MC_MC	682:ARG
685:ARG	HBOND:MC_MC	681:PRO
685:ARG	HBOND:MC_SC	150:SER
685:ARG	HBOND:SC_SC	95:TYR
685:ARG	PICATION:SC_SC	199:TYR
685:ARG	VDW:SC_SC	199:TYR
685:ARG	VDW:SC_SC	192:TYR

To verify the mutation rate among residues of the 675-QTQNSPRRAR-685 region of SARS-CoV-2 S, the protein sequence from Wuhan-Hu-1, China (Accession code: P0DTC2) was used as a reference sequence for the mutation analysis. The NCBI virus database contained 951895 human SARS-CoV-2 S proteins with a protein length between 1233 and 1273 amino acid residues. These represented spike proteins from North America (892185), Europe (22026), Asia (14269), Oceania (11852), South America (7695), and Africa (3868). The protease cleavage site (between residues 675 and 692) in the spike protein is associated with a big mutation density. More than one mutation type can be found at the same position in the spike protein sequence, as shown in Table 2. Interestingly, Arg682, Arg 683, and Arg685 are characterized by the lowest mutation rate, if compared to the other residues of the putative binding motif of SARS-CoV-2 S, with Arg685 being the most conserved, thus corroborating our assumption that Arg685 is the key amino acid in the interaction with the receptor (Table 2).

Table 2. Mutation analysis of the SARS-CoV-2 675-QTQNSPRRAR-685 region. *Freq* values stand for mutation frequency. *WT* and *Mut 1-3* identify, in order, the wild type and the most common mutations.

WT	**Q**	**T**	**Q**	**T**	**N**	**S**	**H**	**R**	**R**	**A**	**R**
Freq	947785	951351	940926	950780	520782	950222	549264	951249	951437	950705	951558
Mut 1	**H**	**I**	**H**	**I**	**K**	**F**	**R**	**W**	**Q**	**V**	**S**
Freq	3727	323	8872	623	429424	239	233082	37	126	605	7
Mut 2	**R**	**A**	**P**	**P**	**T**	**T**	**P**	**L**	**W**	**S**	**H**
Freq	158	79	1595	26	33	153	167824	22	116	103	4
Mut 3	**OTHER**	**OTHER**	**OTHER**	**OTHER**	**OTHER**	**OTHER**	**OTHER**	**OTHER**	**OTHER**	**OTHER**	**OTHER**
Freq	98	43	281	27	77	23	257	13	82	40	3

DISCUSSION

The Covid-19 pandemic caused by infection with SARS-CoV-2 has led to more than 6.8 million deaths worldwide [2]. Several studies have now described the potentially pathological role of macrophages during SARS-CoV-2 infection and discuss possible therapeutic strategies to regulate macrophage activation in patients with Covid-19 [5]. In this scenario, is becoming increasingly evident the role of nAChRs in the clinical manifestations detected in a subset of patients [5]. SARS-CoV-2 S protein has been proposed to potentially interact with nAChRs, based on sequence homology with the

"toxic loop" (loop II) of α-neurotoxins known to bind to these receptors [23]. nAChRs are a well-known target for toxins but also other viruses. Structurally, α-bungarotoxin and other snake toxins share a distinctive three-finger fold characterized by three β-sheeted loops, comprehending the toxic loop II. The viruses and neurotoxins binding motifs entail conserved positively charged amino acid residues (either Arg or Lys) extending away from a loop, which is known to interact with nAChRs [29]. As for α-conotoxins, to date, at least 200 conopeptides have been characterized, which share a common structural α-helical motif that resembles the "toxic loop" of long chain snake toxins [30], including α-bungarotoxin, able to interact with nAChRs and to competitively bind the same region of the receptor [31]. Sequence comparison and secondary structure analysis of SARS-CoV-2 show the presence of features characteristic of the "toxic loop" of α-neurotoxins, namely the cationic moiety but also the typical three-finger fold, which is also found in RABVG and HIV gp-120, suggesting a functional analogy between these proteins.

NMR and X-ray structures of nAChRs and homologous proteins from different species reveal that agonists and competitive antagonists of nAChRs, like α-bungarotoxin and α-conotoxin, bind to the so-called "aromatic box" found in the receptor binding site [29,32,33]. Involved in the binding is a cation-π interaction between a protonated secondary amine of a positive residue of either agonist or antagonist molecules and conserved aromatic residues of the receptor [32]. Since the 682-RRAR-685 putative binding region of SARS-COV-2 S was missing from all the available crystal structures, structure prediction studies were performed to obtain its 3D structure. The interaction between the cationic moiety found on the exposed loop of SARS-CoV-2 S with the aromatic box of the receptor was thus modelled and evaluated after performing MD simulations. We found that that the only conformation possible was the one in which Arg685 of the SARS-CoV-2 hairpin loop fits in the aromatic box of the α9-nAChR subunit. nAChRs binding site is found between one of the α subunits composing the ion channel, named the (+)-interface, and a second accessory subunit named the (-)-interface (either another α subunit or a different one; [32]), where is found the "aromatic box". While agonists seem to be embraced by a closing movement of a loop on the (+)-interface (the loop C) α-neurotoxins seem to push the loop C in a more open conformation [11]. A Trp residue forms a functionally significant cation-π interaction, while the other aromatic residues in the box seem to play an accessory role [32]. According to studies, the Y674-R685 loop of SARS-CoV-2 S protein, which carries the 682-RRAR-685 polybasic motif, is capable of binding three nAChR subtypes, which are the human α4β2 and α7 as well as the muscle-like αβγδ receptor from *Tetronarce californica* [22]. They found that the interaction of the neurotoxin-like region of SARS-CoV-2 with the receptor seems to force loop C into an open conformation, as it happens with nAChR antagonists. Furthermore, their findings indicate that the Y674-R685 peptide is accessible for binding even in the fully glycosylated S protein [22]. Based on these observations, we decided to test the interaction of SARS-CoV-2 S, comprehending not only the 675-QTQNSPRRAR-685 neurotoxin-like region but the whole three-finger portion characterized by the three β-sheeted loops. We found that Arg685 interacts with residues of the α9-nAChR subunit's aromatic box establishing stable interactions, thus corroborating our assumption that, of the three Arg residues in the polybasic region, Arg685 is the key residue for receptor binding. Furthermore, the fact that Arg685 has a very low mutation rate and is highly conserved in the SARS-CoV-2 sequence indicates that it is a functionally relevant residue to the species.

Interestingly, recent studies conducted *in vitro* have confirmed the involvement of the 675-QTQNSPRRAR-685 region of SARS-CoV-2 in the modulation of the cholinergic response [21]. They applied whole-cell and single-channel recordings to determine whether a peptide corresponding to the Y674-R685 region of the S protein could affect α7 nAChR function. They found that the fragment can activate α7-nAChRs in the presence of positive allosteric modulators, but also exerts a negative modulation of α7. As mentioned above, increased release of ACh from the vagus nerve in response to endogenous or exogenous stimuli triggers the activation of nAChRs on the macrophage cell membrane, reducing the production of inflammatory cytokines and, as a result, inhibiting inflammation [10]. Consequently, the work from Chrestia et al., provides proof of a possible effect of the SARS-CoV-2 on the cytokine storm production triggered by the cholinergic blockade [21] by interfering with the activation of the nAChRs.

METHODS

4.1. Structural analysis

The primary sequences of SARS-COV-2 Spike protein, α-bungarotoxin, α-conotoxin, RABVG, and gp120 HIV were retrieved from the UniProt database [34], with accession numbers P0DTC2, P60615, P01519, O92284, P04578 respectively.

All available crystal structures of selected proteins were downloaded from the RCBS Protein Data Bank (www.rcsb.org). Three-dimensional atomic coordinates of the missing loop 682-685 of SARS-COV-2 Spike protein were generated by using MODELLER implemented in PyMod 2.0 [35]. The Uniprot ID P04578 sequence of HIV-1 gp120 was generated with Phyre 2 by using as template PDB ID 6B0N [36].

Electrostatic potential maps were numerically computed solving the PB equation with default settings using the PBEQ Solver within CHARMM-GUI [37] and graphed using Chimera [38].

4.2. MD simulations

Molecular dynamics (MD) simulations were carried out in GROMACS 2019 [39]. The protein structures were solvated in a triclinic box filled with 33766 TIP3P water molecules, adding 112 Na+ and 96 Cl- ions to neutralize the system at a concentration of 0,15 M. The whole systems were then minimized with a maximal force tolerance of 1000 kJ mol-1 nm-1 using the steepest descendent algorithm. The optimized systems were gradually heated to 300 K in 1 ns in the NVT ensemble, followed by 10 ns equilibration in the NPT ensemble at 1 Atm and 300 K, using the V-Rescale thermostat and Berendsen barostat [40, 41], with Cα atoms restrained. Newton's equations of atomic motion were integrated by the Verlet algorithm with a 2 fs time step. LINCS algorithm [42] to constrain all the covalent bonds involving hydrogen atoms and the Particle Mesh Ewald (PME) algorithm was employed for long-range interactions computation [43]. The analysis tools implemented in GROMACS were applied to calculate Root-mean-square deviation (RMSD).

4.3. Residue Interaction Network (RIN) analysis

The RIN was constructed by submitting the average structure extracted from the equilibrium phase of the MD simulation trajectory to the RING 2.0 web server (http://protein.bio.unipd.it/ring/). RING enables to analyze of mutation effects, protein folding, domain–domain communication, and catalytic activity through the identification of covalent and non-covalent bonds in protein structures, including π–π stacking and π–cation interactions [44].

4.4. Mutation Analysis

The SARS-CoV-2 spike protein sequences were obtained in the FASTA format from the NCBI virus database (https://www.ncbi. nlm.nih.gov/labs/virus/vssi/). The multiple sequence alignment of the spike proteins was achieved using Clustal Omega (https://www.ebi.ac.uk/Tools/msa/clustalo/). The human SARS-CoV-2 spike protein sequence from Wuhan-Hu-1, China (Accession code: P0DTC2) was used as a reference sequence to examine the mutations in a motif contained in the spike protein. The mutations were analyzed according to their presence within different regions of the spike protein sequence.

CONCLUSIONS

nAChRs are well-known targets for toxins but also viruses. Our results suggest that SARS-CoV-2 S protein can bind nAChRs through stable interactions between a region containing the 682-RRAR-685 polybasic insertion typical of SARS-CoV-2 but that was absent in other coronaviruses. This motif is found in a region with high sequence similarity with neurotoxins known to bind nAChRs. Sequence comparison with the “toxic loop” of α-bungarotoxin and RABVG neurotoxin-like region, as well as HIV-1 gp20 and α-conotoxin from *Conus geographus*, highlights the existence of a correlation between these proteins’ functional sites. Secondary structure analysis, along with electrostatic potential calculations, unveiled the presence of features characteristic of the “toxic loop”, and the same observations can be done for RABVG and HIV-1 gp-120, suggesting a functional analogy between these different proteins. Finally, MD simulations and Residue Interaction Network analyses confirmed our hypothesis that the neurotoxin-like region found in the SARS-CoV-2 S protein might be involved in the binding to nAChRs, underlying the key role of Arg685 amino acid residue in the interaction, where the guanidinium group serves as a crucial point of attachment to the receptor “aromatic box”. These findings may be relevant to understanding Covid-19 pathophysiology and infection and could be a guide for the development of future novel therapeutic strategies.

REFERENCES

I. Huang, C.; Wang, Y.; Li, X.; Ren, L.; Zhao, J.; Hu, Y.; Zhang, L.; Fan, G.; Xu, J.; Gu, X.; et al. Clinical Features of Patients Infected with 2019 Novel Coronavirus in Wuhan, China. *Lancet* 2020, *395*, 497–506, doi:10.1016/S0140-6736(20)30183-5. Https://Covid19.Who.Int/.

II. Hu, B.; Guo, H.; Zhou, P.; Shi, Z.-L. Characteristics of SARS-CoV-2 and COVID-19., doi:10.1038/s41579-020-00459-7.

III. Hoffmann, M.; Kleine-Weber, H.; Schroeder, S.; Krüger, N.; Herrler, T.; Erichsen, S.; Schiergens, T.S.; Herrler, G.; Wu, N.-H.; Nitsche, A.; et al. SARS-CoV-2 Cell Entry Depends on ACE2 and TMPRSS2 and Is Blocked by a Clinically Proven Protease Inhibitor. *Cell* 2020, *181*, 271-280.e8, doi:10.1016/j.cell.2020.02.052.

IV. Kopańska, M.; Batoryna, M.; Bartman, P.; Szczygielski, J.; Banaś-Ząbczyk, A. Disorders of the Cholinergic System in COVID-19 Era—A Review of the Latest Research. *Int J Mol Sci* 2022, *23*, 672, doi:10.3390/ijms23020672.

V. Coutard, B.; Valle, C.; de Lamballerie, X.; Canard, B.; Seidah, N.G.; Decroly, E. The Spike Glycoprotein of the New Coronavirus 2019-NCoV Contains a Furin-like Cleavage Site Absent in CoV of the Same Clade. *Antiviral Res* 2020, *176*, doi:10.1016/J.ANTIVIRAL.2020.104742.

VI. Fu, Y.; Cheng, Y.; Wu, Y. Understanding SARS-CoV-2-Mediated Inflammatory Responses: From Mechanisms to Potential Therapeutic Tools. *Virol Sin* 2020, *35*, 266–271, doi:10.1007/s12250-020-00207-4.

VII. Gharpure, A.; Noviello, C.M.; Hibbs, R.E. Progress in Nicotinic Receptor Structural Biology. *Neuropharmacology* 2020, *171*, 108086, doi:10.1016/j.neuropharm.2020.108086.

VIII. Hecker, A.; Küllmar, M.; Wilker, S.; Richter, K.; Zakrzewicz, A.; Atanasova, S.; Mathes, V.; Timm, T.; Lerner, S.; Klein, J.; et al. Phosphocholine-Modified Macromolecules and Canonical Nicotinic Agonists Inhibit ATP-Induced IL-1β Release. *J Immunol* 2015, *195*, 2325–2334, doi:10.4049/jimmunol.1400974.

IX. Kruk-Słomka, M.; Budzyńska, B.; Biała, G. Involvement of Cholinergic Receptors in the Different Stages of Memory Measured in the Modified Elevated plus Maze Test in Mice. *Pharmacological Reports* 2012, *64*, 1066–1080, doi:10.1016/S1734-1140(12)70904-0.

X. Dutertre, S.; Nicke, A.; Tsetlin, V.I. Nicotinic Acetylcholine Receptor Inhibitors Derived from Snake and Snail Venoms. *Neuropharmacology* 2017, *127*, 196–223, doi:10.1016/j.neuropharm.2017.06.011.

XI. Endo, T.; Tamiya, N. Current View on the Structure-Function Relationship of Postsynaptic Neurotoxins from Snake Venoms. *Pharmacol Ther* 1987, *34*, 403–406, doi:10.1016/0163-7258(87)90002-7.

XII. Neri, P.; Bracci, L.; Rustici, M.; Santucci, A. Sequence Homology between HIV Gp120, Rabies Virus Glycoprotein, and Snake Venom Neurotoxins. *Arch Virol* 1990, *114*, 265–269, doi:10.1007/BF01310756.

XIII. Bracci, L.; Lozzi, L.; Rustici, M.; Neri, P. Binding of HIV-1 Gp120 to the Nicotinic Receptor. *FEBS Lett* 1992, *311*, 115–118, doi:10.1016/0014-5793(92)81380-5.

XIV. Sajjanar, B.; Dhusia, K.; Saxena, S.; Joshi, V.; Bisht, D.; Thakuria, D.; Manjunathareddy, G.B.; Ramteke, P.W.; Kumar, S. Nicotinic Acetylcholine Receptor Alpha 1(NAChRα1) Subunit Peptides as Potential Antiviral Agents against Rabies Virus. *Int J Biol Macromol* 2017, *104*, 180–188, doi:10.1016/j.ijbiomac.2017.05.179.

XV. Lentz, T.L. Structure-Function Relationships of Curaremimetic Neurotoxin Loop 2 and of a Structurally Similar Segment of Rabies Virus Glycoprotein in Their Interaction with the Nicotinic Acetylcholine Receptor. *Biochemistry* 1991, *30*, 10949–10957, doi:10.1021/bi00109a020.

XVI. Jackson, A.C. Current and Future Approaches to the Therapy of Human Rabies. *Antiviral Res* 2013, *99*, 61–67, doi:10.1016/J.ANTIVIRAL.2013.01.003.

XVII. Skok, M. v.; Grailhe, R.; Agenes, F.; Changeux, J.P. The Role of Nicotinic Receptors in B-Lymphocyte Development and Activation. *Life Sci* 2007, *80*, 2334–2336, doi:10.1016/J.LFS.2007.02.005.

XVIII. Kawashima, K.; Fujii, T.; Moriwaki, Y.; Misawa, H.; Horiguchi, K. Non-Neuronal Cholinergic System in Regulation of Immune Function with a Focus on A7 NAChRs. *Int Immunopharmacol* 2015, *29*, 127–134, doi:10.1016/j.intimp.2015.04.015.

XIX. Valdés-Ferrer, S.I.; Crispín, J.C.; Belaunzarán-Zamudio, P.F.; Rodríguez-Osorio, C.A.; Cacho-Díaz, B.; Alcocer-Varela, J.; Cantú-Brito, C.; Sierra-Madero, J. Add-on Pyridostigmine Enhances CD4+ T-Cell Recovery in HIV-1-Infected Immunological Non-Responders: A Proof-of-Concept Study. *Front Immunol* 2017, *8*, doi:10.3389/fimmu.2017.01301.

XX. Chrestia, J.F.; Oliveira, A.S.; Mulholland, A.J.; Gallagher, T.; Bermúdez, I.; Bouzat, C. A Functional Interaction Between Y674-R685 Region of the SARS-CoV-2 Spike Protein and the Human A7 Nicotinic Receptor. *Mol Neurobiol* 2022, *59*, 6076–6090, doi:10.1007/s12035-022-02947-8.

XXI. Oliveira, A.S.F.; Ibarra, A.A.; Bermudez, I.; Casalino, L.; Gaieb, Z.; Shoemark, D.K.; Gallagher, T.; Sessions, R.B.; Amaro, R.E.; Mulholland, A.J. A Potential Interaction between the SARS-CoV-2 Spike Protein and Nicotinic Acetylcholine Receptors. *Biophys J* 2021, *120*, 983–993, doi:10.1016/J.BPJ.2021.01.037.

XXII. Changeux, J.-P.; Amoura, Z.; Rey, F.A.; Miyara, M. A Nicotinic Hypothesis for Covid-19 with Preventive and Therapeutic Implications. *C R Biol* 2020, *343*, 33–39, doi:10.5802/crbiol.8.

XXIII. Dormoy, V.; Perotin, J.M.; Gosset, P.; Maskos, U.; Polette, M.; Deslée, G. Nicotinic Receptors as SARS-CoV-2 Spike Co-Receptors? *Med Hypotheses* 2022, *158*, doi:10.1016/J.MEHY.2021.110741.

XXIV. Lagoumintzis, G.; Chasapis, C.T.; Alexandris, N.; Kouretas, D.; Tzartos, S.; Eliopoulos, E.; Farsalinos, K.; Poulas, K. Nicotinic Cholinergic System and COVID-19: In Silico Identification of Interactions between A7 Nicotinic Acetylcholine Receptor and the Cryptic Epitopes of SARS-Co-V and SARS-CoV-2 Spike Glycoproteins. *Food and Chemical Toxicology* 2021, *149*, 112009, doi:10.1016/J.FCT.2021.112009.

XXV. Doria, D.; Santin, A.D.; Tuszynski, J.A.; Scheim, D.E.; Aminpour, M. Omicron SARS-CoV-2 Spike-1 Protein’s Decreased Binding Affinity to α7nAChr: Implications for Autonomic Dysregulation of the Parasympathetic Nervous System and the Cholinergic Anti-Inflammatory Pathway—An In Silico Analysis. *BioMedInformatics 2022, Vol. 2, Pages 553-564* 2022, *2*, 553–564, doi:10.3390/BIOMEDINFORMATICS2040035.

XXVI. Kalashnyk, O.; Lykhmus, O.; Izmailov, M.; Koval, L.; Komisarenko, S.; Skok, M. SARS-Cov-2 Spike Protein Fragment 674e685 Protects Mitochondria from Releasing Cytochrome c in Response to Apoptogenic Influence. 2021, doi:10.1016/j.bbrc.2021.05.018.

XXVII. Wang, H.-L.; Gao, F.; Bren, N.; Sine, S.M. Curariform Antagonists Bind in Different Orientations to the Nicotinic Receptor Ligand Binding Domain. *Journal of Biological Chemistry* 2003, *278*, 32284–32291, doi:10.1074/jbc.M304366200.

XXVIII. Scarselli, M.; Spiga, O.; Ciutti, A.; Bernini, A.; Bracci, L.; Lelli, B.; Lozzi, L.; Calamandrei, D.; di Maro, D.; Klein, S.; et al. NMR Structure of α-Bungarotoxin Free and Bound to a Mimotope of the Nicotinic Acetylcholine Receptor. *Biochemistry* 2002, *41*, 1457–1463, doi:10.1021/BI011012F.

XXIX. Servent, D.; Thanh, H.L.; Antil, S.; Bertrand, D.; Corringer, P.J.; Changeux, J.P.; Ménez, A. Functional Determinants by Which Snake and Cone Snail Toxins Block the A7 Neuronal Nicotinic Acetylcholine Receptors. *J Physiol Paris* 1998, *92*, 107–111, doi:10.1016/S0928-4257(98)80146-0.

XXX. Cecchini, M.; Changeux, J.P. The Nicotinic Acetylcholine Receptor and Its Prokaryotic Homologues: Structure, Conformational Transitions & Allosteric Modulation. *Neuropharmacology* 2015,

96, 137–149, doi:10.1016/J.NEUROPHARM.2014.12.006.

XXXI. Post, M.R.; Tender, G.S.; Lester, H.A.; Dougherty, D.A. Secondary Ammonium Agonists Make Dual Cation-π Interactions in A4β2 Nicotinic Receptors. *eNeuro* 2017, *4*, ENEURO.0032-17.2017, doi:10.1523/ENEURO.0032-17.2017.

XXXII. Morales Duque, H.; Campos Dias, S.; Franco, O. Structural and Functional Analyses of Cone Snail Toxins. *Mar Drugs* 2019, *17*, 370, doi:10.3390/md17060370.

XXXIII. Bateman, A.; Martin, M.J.; O'Donovan, C.; Magrane, M.; Alpi, E.; Antunes, R.; Bely, B.; Bingley, M.; Bonilla, C.; Britto, R.; et al. UniProt: The Universal Protein Knowledgebase. *Nucleic Acids Res* 2017, *45*, D158–D169, doi:10.1093/NAR/GKW1099.

XXXIV. Webb B, Sali A. Protein Structure Modeling with MODELLER. Methods Mol Biol. 2017;1654:39-54. doi: 10.1007/978-1-4939-7231-9_4. PMID: 28986782

XXXV. Kelley LA et al.. Nature Protocols 10, 845-858 (2015)

XXXVI. Jo, S.; Kim, T.; Iyer, V.G.; Im, W. CHARMM-GUI: A Web-Based Graphical User Interface for CHARMM. *J Comput Chem* 2008, *29*, 1859–1865, doi:10.1002/jcc.20945.

XXXVII. Pettersen, E.F.; Goddard, T.D.; Huang, C.C.; Couch, G.S.; Greenblatt, D.M.; Meng, E.C.; Ferrin, T.E. UCSF Chimera—A Visualization System for Exploratory Research and Analysis. *J Comput Chem* 2004, *25*, 1605–1612, doi:10.1002/JCC.20084.

XXXVIII. Abraham, M.J.; Murtola, T.; Schulz, R.; Páll, S.; Smith, J.C.; Hess, B.; Lindah, E. Gromacs: High Performance Molecular Simulations through Multi-Level Parallelism from Laptops to Supercomputers. *SoftwareX* 2015, *1–2*, 19–25, doi:10.1016/J.SOFTX.2015.06.001.

XXXIX. Bussi, G.; Donadio, D.; Parrinello, M. Canonical Sampling through Velocity Rescaling. *J Chem Phys* 2007, *126*, 014101, doi:10.1063/1.2408420.

XL. Berendsen, H.J.C.; Postma, J.P.M.; van Gunsteren, W.F.; DiNola, A.; Haak, J.R. Molecular Dynamics with Coupling to an External Bath. *J Chem Phys* 1984, *81*, 3684–3690, doi:10.1063/1.448118.

XLI. Hess, B.; Bekker, H.; C Berendsen, H.J.; E M Fraaije, J.G. 3 LINCS: A Linear Constraint Solver for Molecular Simulations. 1997, *18*, 1463–1472.

XLII. Darden, T.; York, D.; Pedersen, L. Particle Mesh Ewald: An N⋅Log(N) Method for Ewald Sums in Large Systems. *J Chem Phys* 1993, *98*, 5648, doi:10.1063/1.464397.

XLIII. Piovesan, D.; Minervini, G.; Tosatto, S.C.E. The RING 2.0 Web Server for High Quality Residue Interaction Networks. *Nucleic Acids Res* 2016, *44*, W367–W374, doi:10.1093/nar/gkw315.